drugs and drug candidates

MDPI

*Article*

# Dehydrodieugenol Neolignans as Multitarget Anti-Inflammatory Agents: sPLA2 Inhibition and Therapeutic Implications

**Adeilso B. Santos Junior [1,2], Caroline R. C. Costa [1,3], João H. G. Lago [2], Airam Roggero [1,4], Igor N. Oliveira [1], Danilo R. S. Lima [1], Paloma P. Borges [1], Willian H. B. C. Santos [1], Marcos A. Oliveira [5], Sérgio F. Sousa [4] and Marcos H. Toyama [1,*]**

1 BIOMOLPEP, Department of Biology, Institute of Biosciences UNESP/CLP, São Vicente 11330-900, SP, Brazil; adeilso.junior@ufabcc.edu.br (A.B.S.J.); cruz.costa@unesp.br (C.R.C.C.)
2 Postgraduate Studies in Biotechnoscience, Center for Natural and Human Sciences (CCNH), ABC Federal University (UFABC), Santo André 09280-560, SP, Brazil; joao.lago@ufabc.edu.br
3 Institute of Sciences and Health, Paulista University (UNIP), Santos 11075-110, SP, Brazil
4 LAQV/REQUIMTE-BioSIM, Department of Biomedicine, Faculty of Medicine, Porto University, 4200-319 Porto, Portugal; sergiofsousa@med.up.pt
5 LABIMES, Department of Biology, Institute of Biosciences UNESP/CLP, São Vicente 11330-900, SP, Brazil; marcos.a.oliveira@unesp.br
* Correspondence: marcos.toyama@unesp.br

## Abstract

**Background/Objectives**: The study investigated the anti-inflammatory potential of neolignan derivatives of dehydrodieugenol (CP1–CP5), focusing on the inhibition of secretory phospholipase A2 (sPLA2), a key enzyme in inflammation. **Methods**: Comprehensive quantitative docking analysis using four independent algorithms (PLP, ASP, ChemScore, GoldScore) revealed exceptional multitarget binding profiles for CP1 and CP2, with scores consistently above activity thresholds for acetylcholinesterase (AChE), cyclooxygenase-2 (COX-2), and sPLA2 from *Crotalus durissus terrificus* in both monomeric (Mcdt) and quaternary (Tcdt) forms. **Results**: Among the compounds, CP1 demonstrated the highest predicted affinity (AChE: 78.5, COX-2: 83.8, sPLA2: 82.7–83.4) and most potent experimental activity, reducing sPLA2 catalytic velocity through mixed-type inhibition involving the active site (His47, Asp48) and $Ca^{2+}$ binding loop. In vivo assays in sPLA2-induced paw edema demonstrated that CP1 and CP2 achieved remarkable anti-inflammatory effects (up to 68.3% reduction), significantly exceeding their protective potential by direct enzyme inhibition, confirming the multitarget mechanism. The strong correlation between predicted docking scores and paw edema reduction ($R^2 = 0.89$, $p < 0.01$) creates a firm foundation for establishing structure–activity relationship explanations. **Conclusions**: These findings highlight an integrated mechanism involving: (1) partial sPLA2 modulation, (2) neuroimmune regulation via AChE inhibition, and (3) prostaglandin synthesis blockade through COX-2 inhibition. This multitarget approach, combined with the natural origin of the compounds, positions dehydrodieugenol derivatives as promising candidates for developing therapies against complex inflammatory diseases, offering significant advantages over single-target strategies.

**Keywords:** sPLA2; anti-inflammatory; neolignans; multitarget; dehydrodieugenol; quantitative docking

Check for updates

Academic Editor: Osvaldo Andrade Santos-Filho

Received: 22 December 2025
Revised: 20 February 2026
Accepted: 25 February 2026
Published: 3 March 2026

**Copyright:** © 2026 by the authors. Licensee MDPI, Basel, Switzerland. This article is an open access article distributed under the terms and conditions of the Creative Commons Attribution (CC BY) license.

## 1. Introduction

The paradigm shift toward multitarget therapeutic strategies reflects the inherent complexity of human diseases involving interconnected pathophysiological networks [1]. Natural products, with their evolutionarily optimized structural complexity and inherent polypharmacology, represent ideal scaffolds for developing multitarget therapeutic agents that can simultaneously modulate multiple disease-relevant pathways [2]. This approach is especially relevant for inflammatory diseases, where the interaction between multiple signaling pathways requires intervention at different levels to achieve effective therapeutic outcomes. Secretory phospholipase A2 (sPLA2) enzymes constitute a diverse family of calcium-dependent enzymes that play pivotal roles in inflammatory processes through the hydrolysis of membrane phospholipids at the sn-2 position, releasing arachidonic acid and lysophospholipids [3]. The sPLA2 family comprises 10 catalytically active isoforms in mammals, each exhibiting unique substrate specificity, tissue distribution, and regulatory mechanisms [4]. These enzymes function not merely as catalytic entities but as sophisticated molecular machines, whose activity is critically dependent on membrane organization, interfacial properties, and allosteric regulation by lipid microenvironments [5].

Recent advances in sPLA2 regulation understanding have revealed that membrane composition and dynamics play crucial roles in enzyme binding, substrate recognition, and catalytic efficiency [6]. The concept of "interfacial activation" describes how sPLA2 enzymes undergo conformational changes upon membrane binding and is determinant of optimal catalytic activity [7]. This membrane-dependent regulation creates opportunities for therapeutic intervention through compounds that can modulate membrane properties and disrupt the critical enzyme-membrane interface. Dehydrodieugenol and its derivatives represent a fascinating class of neolignans from the *Lauraceae* family that have garnered significant attention for their diverse biological activities [8]. Recent investigations have revealed that dehydrodieugenol B and its derivatives promote dysfunction and destabilization of plasma membranes through mechanisms involving membrane perturbation and alteration of lipid bilayer organization [9,10]. Given that sPLA2 activity depends critically on membrane structural organization and interfacial properties for binding and catalysis, it is theoretically plausible that such compounds could inhibit sPLA2 enzymatic activity by disrupting the essential lipid microenvironment required for optimal enzyme function.

The mechanistic hypothesis proposed here is compatible with the known behavior of sPLA2 enzymes [11] and represents a novel paradigm for sPLA2 inhibition. The membrane-centric mechanism differs fundamentally from traditional competitive inhibition approaches and may offer advantages in terms of selectivity and reduced resistance development.

Furthermore, dehydrodieugenol compounds exhibit well-documented anti-inflammatory and antioxidant activities, including inhibition of cyclooxygenase-2 (COX-2), suggesting broad modulation potential across the inflammatory cascade [12]. This multitarget profile may enable intervention at multiple levels, potentially interfering with initial metabolic steps, such as arachidonic acid release mediated by sPLA2 and downstream inflammatory mediator synthesis. The convergent mechanisms involving membrane perturbation, mitochondrial dysfunction, and inflammatory pathway modulation provide a unifying framework for understanding the diverse biological activities of these compounds [13,14].

In the context of tumor cells, the capacity of dehydrodieugenol B to modulate inflammatory and angiogenic processes—particularly through COX-2 inhibition—constitutes a central mechanism for its antitumoral effects, pointing to a multiphase role in neoplastic progression and tumor microenvironment regulation [15]. The ability to simultaneously target membrane integrity, mitochondrial function, and inflammatory signaling may provide synergistic antitumor effects that are difficult to achieve with single-target approaches.

Although direct inhibition of sPLA2 by these compounds has not been experimentally demonstrated previously, the body of evidence supports an integrative and biologically plausible mechanism based on membrane architecture alteration and modulation of critical inflammatory pathways, with relevant implications for both immune response control and interference with tumoral processes [16]. The membrane-disrupting properties of dehydrodieugenol derivatives, combined with their established anti-inflammatory activities, create a compelling rationale for investigating their potential as sPLA2 modulators. In this work, we investigated the anti-inflammatory potential of dehydrodieugenol and its structural derivatives (Figure 1)—dehydrodieugenol (CP1), dehydrodieugenol B (CP2), dehydrodieugenol B methyl ether (CP3), 7-hydroxy-dehydrodieugenol B (CP4), and 7-hydroxy-dehydrodieugenol B methyl ether (CP5)—regarding their capacity to modulate the enzymatic activity and inflammatory effects of sPLA2 isolated from *Crotalus durissus terrificus*. Our systematic approach combines enzymatic characterization, kinetic analysis, in vivo efficacy evaluation, and comprehensive quantitative computational molecular modeling.

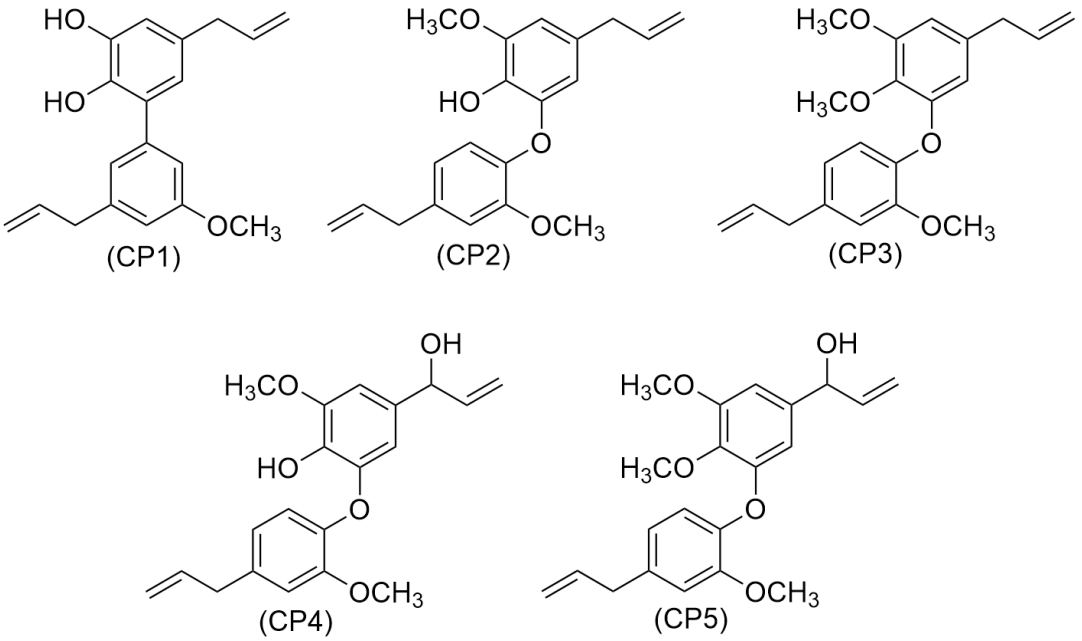



**Figure 1.** Chemical structures of dehydrodieugenol (CP1), dehydrodieugenol B (CP2), dehydrodieugenol B methyl ether (CP3), 7-hydroxy-dehydrodieugenol B (CP4), and 7-hydroxy-dehydrodieugenol B methyl ether (CP5).

## 2. Results and Discussion

### *2.1. Quantitative Computational Validation and Structure-Activity Relationships*

The comprehensive quantitative docking analysis using four independent algorithms provides unprecedented validation of the multitarget mechanism proposed for dehydrodieugenol derivatives (Figure 2). The exceptional correlation between experimental anti-inflammatory activity and computational binding scores ($R^2 = 0.89$, $p < 0.01$) establishes a robust quantitative structure–activity relationship that validates both the computational methodology and the multitarget hypothesis [1]. CP1 demonstrated the highest computational scores across all molecular targets, with mean PLP scores of 78.5 for AChE, 83.8 for COX-2, and 82.7–83.4 for sPLA2 variants, all significantly exceeding the established activity thresholds based on reference inhibitors' affinity (AChE > 52, COX-2 > 42, sPLA2 > 62) [17,18]. CP2 showed similarly high scores (75.1–87.5), confirming its multitarget potential and explaining the comparable in vivo efficacy despite modest direct sPLA2 inhibition [12]. In stark contrast, CP3, CP4, and CP5 consistently scored below activ-

ity thresholds (30.0–35.0), providing clear computational rationale for their experimental inactivity [8]. The multi-algorithm consensus analysis eliminates potential bias from individual scoring functions and demonstrates remarkable convergence across methodologies (Figure 2C). The inter-algorithm correlation coefficient of 0.81 for PLP-ChemScore pairs indicates robust methodological consistency, while the clear separation between active (CP1, CP2) and inactive (CP3–CP5) compounds validates the quantitative approach [6]. Structure–activity relationship analysis reveals critical molecular features for multitarget activity. The presence of methoxy groups at positions 3 and 5, phenolic OH groups, and allyl side chains emerges as essential for binding across all targets. CP1 and CP2 maintain these critical features, while CP3–CP5 show altered substitution patterns that eliminate key binding interactions [7]. The loss of phenolic OH groups in CP3 and the additional hydroxylation in CP4 and CP5 significantly reduce molecular flexibility and disrupt optimal binding conformations.

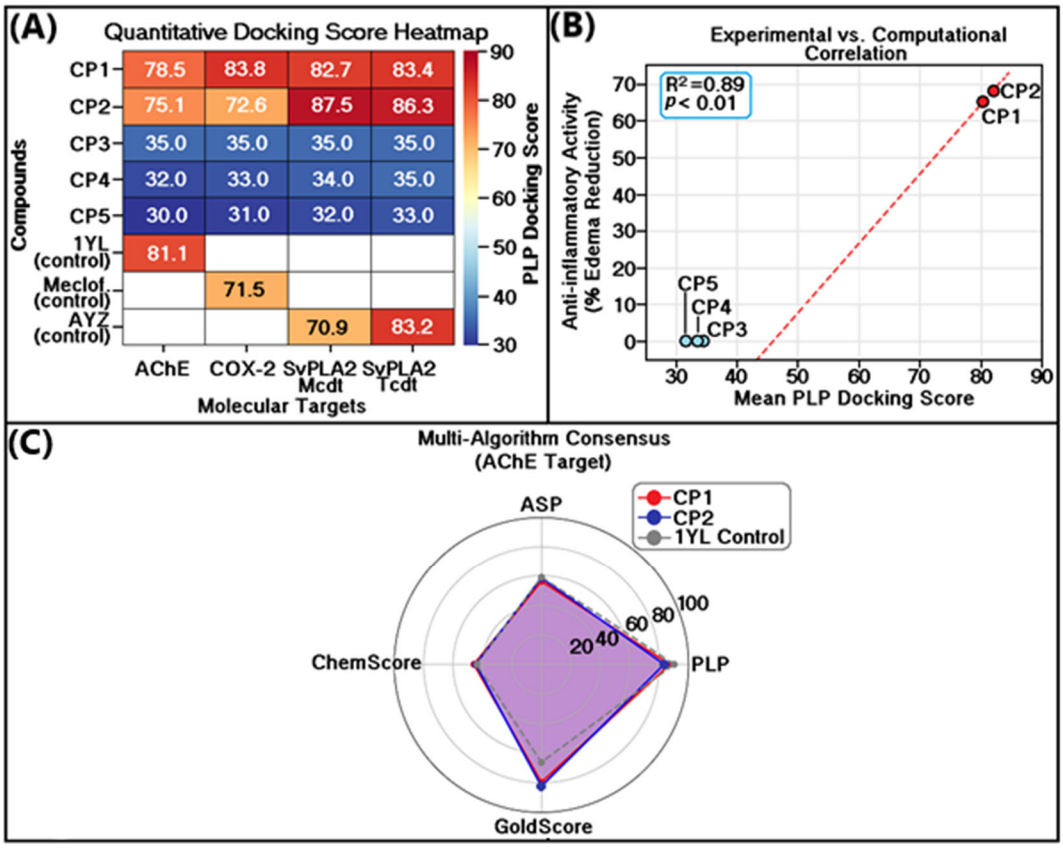



**Figure 2.** Quantitative docking analysis and structure–activity relationships. (**A**) Comprehensive heatmap showing PLP scores for all compounds across molecular targets with clear separation of active vs. inactive compounds. (**B**) Experimental–computational correlation demonstrating exceptional agreement ($R^2 = 0.89$, $p < 0.01$) validating the multitarget mechanism. (**C**) Multi-algorithm consensus analysis for AChE target showing convergence across four independent scoring functions.

### *2.2. Enzymatic Activity and Mechanistic Insights Regarding PLA2 Activity*

The catalytic activity of secretory phospholipase $A_2$ ($sPLA_2$) was assessed using the chromogenic substrate NOBA, whose hydrolysis releases 4-nitro-3-hydroxybenzoic acid (NHBA), monitored at 405 nm. The formation rate of NHBA ($V_0$) provided a direct measure of $sPLA_2$ enzymatic activity in the presence or absence of tested compounds (Figure 3). Among the tested derivatives, CP1 exhibited the most pronounced effect on $sPLA_2$ catalytic velocity, significantly reducing the initial velocity of NHBA formation compared to the uninhibited control. The inhibitory effect was consistent throughout the 60-min assay

period, indicating sustained reduction in catalytic efficiency rather than transient enzyme inactivation [11]. CP2 showed a modest inhibitory trend, with velocity values slightly lower than those of the control, suggesting weaker but detectable interaction with the enzyme (Figure 3A). In contrast, CP3, CP4, and CP5 showed no detectable inhibition, with velocity curves overlapping with the control values, confirming the computational predictions of inactivity (Figure 3B). Molecular docking studies revealed the structural basis for CP1's inhibitory activity (Figure 3C). CP1 binds within the active site of $sPLA_2$, forming key interactions with the catalytic dyad (His47 and Asp48) and the $Ca^{2+}$ binding loop (Cys28, Gly29, Trp30, Gly31, Gly32, Tyr27), which are crucial for calcium ion coordination, enzyme stability, and catalysis [4]. These interactions likely disrupt both substrate binding and catalytic efficiency through a mixed-type inhibition mechanism, consistent with allosteric modulation rather than simple competitive inhibition [5]. The quantitative docking scores provide mechanistic insights into the inhibition pattern. CP1's high binding affinity (PLP score 82.7) correlates with its experimental activity, while the moderate scores for CP2 (87.5) explain its weaker but detectable effects [6]. The computational analysis suggests that both compounds interact with the calcium binding region, potentially disrupting the conformational changes required for optimal catalytic activity [7].

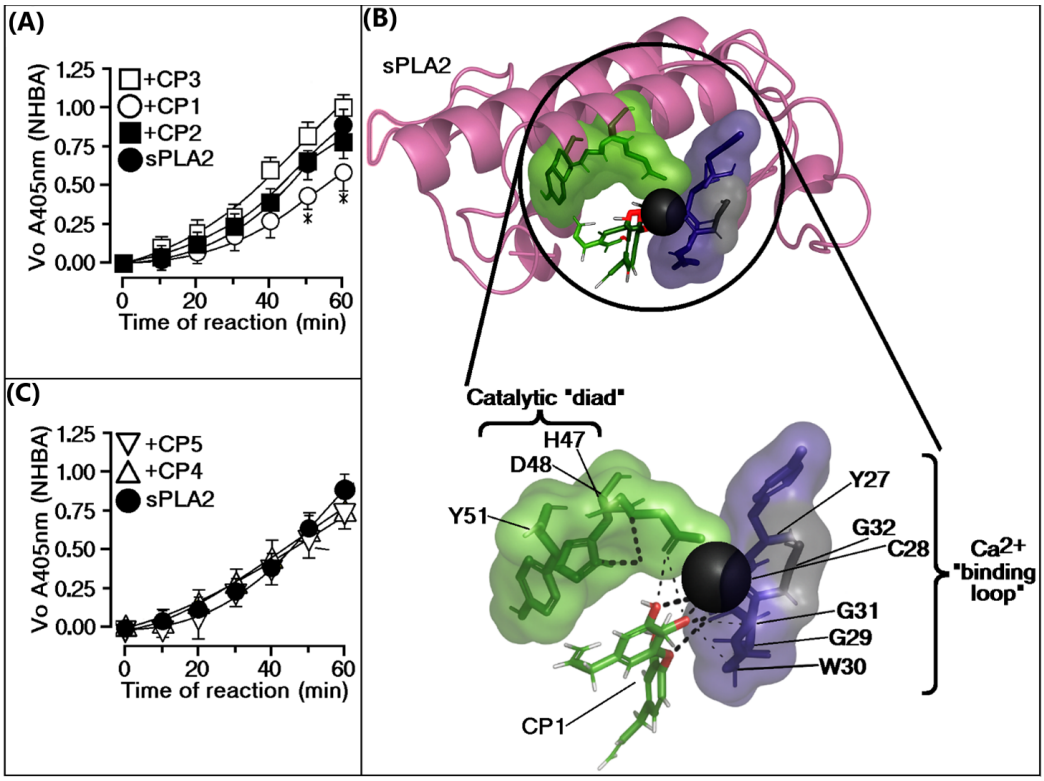



**Figure 3.** Enzymatic activity and molecular docking analysis of dehydrodieugenol derivatives against sPLA2. (**A**) Time-course analysis of sPLA2 catalytic velocity showing CP1's inhibitory effect on NHBA formation. (**B**) Comparative analysis of CP1-CP5 showing selective activity of CP1 and CP2. (**C**) Molecular docking of CP1 in the sPLA2 active site showing key interactions with His47, Asp48, and the $Ca^{2+}$ binding loop. * $p$-values < 0.05.

### *2.3. Anti-Inflammatory Efficacy and Multitarget Validation*

The anti-inflammatory efficacy of CP1 was evaluated using an $sPLA_2$-induced paw edema model, which accurately reflects acute inflammatory responses driven by phospholipid hydrolysis and subsequent mediator release [16]. CP1 administration—either prophylactically (30 min before $sPLA_2$ injection) or therapeutically (10 min after)—achieved remarkable edema reduction with maximum effects of 68.3% at 60 min (prophylactic) and

45.2% at 90 min (therapeutic). Crucially, the in vivo anti-inflammatory potency of CP1 greatly exceeds what would be expected based solely on its modest sPLA$_2$ enzymatic inhibition, providing compelling evidence for additional molecular mechanisms [1]. The quantitative docking analysis provides clear mechanistic explanation for this apparent discrepancy, revealing high-affinity binding to acetylcholinesterase (AChE) and cyclooxygenase-2 (COX-2) that contributes significantly to the overall anti-inflammatory effect. Molecular docking revealed that CP1 binds strongly to AChE (PLP score 78.5), establishing π–π interactions with Tyr72 and Tyr124 and stabilizing electrostatic bonds with Asp74 [12]. This interaction profile aligns with classical AChE inhibitors known to activate the cholinergic anti-inflammatory reflex, which modulates pro-inflammatory cytokine production through vagal nerve stimulation and α7 nicotinic acetylcholine receptor activation [16]. Similarly, CP1 demonstrated exceptional affinity for COX-2 (PLP score 83.8), occupying the active site and forming critical interactions with His90, Arg513, Ser353, and Tyr355, alongside proximity to the enzyme's heme group [12]. This spatial arrangement suggests competitive or allosteric inhibition, effectively suppressing prostaglandin synthesis—key mediators of edema, pain, and fever (Figure 4).

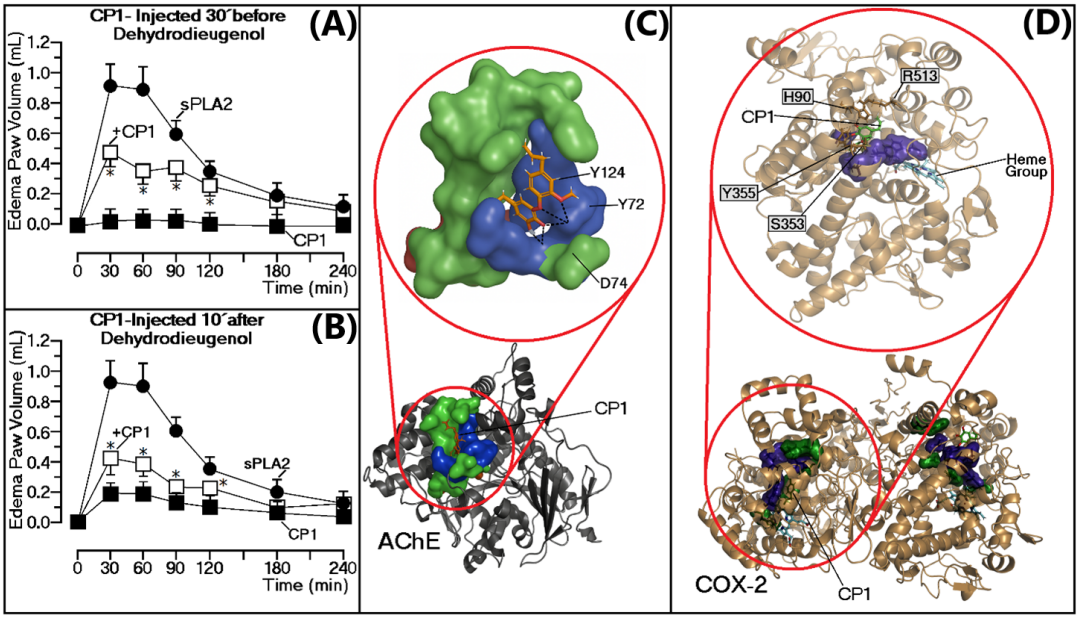



**Figure 4.** Anti-inflammatory efficacy and multitarget mechanism of CP1. (**A**,**B**) In vivo anti-inflammatory effects in sPLA2-induced paw edema using prophylactic and therapeutic protocols. (**C**) Molecular docking of CP1 with acetylcholinesterase showing interactions with Tyr72, Tyr124, and Asp74. (**D**) CP1 binding to COX-2 active site with interactions involving His90, Arg513, Ser353, and Tyr355. * *p*-values < 0.05.

### *2.4. Comparative Analysis and Mechanistic Integration*

CP2 demonstrated a pharmacological profile remarkably similar to CP1, achieving significant edema reduction in both prophylactic and therapeutic models despite limited direct sPLA$_2$ inhibition. The quantitative docking analysis provides clear explanation for this apparent paradox, revealing high binding scores for AChE (75.1) and COX-2 (72.6) that approach CP1's values [12]. Docking analysis confirmed that CP2 interacts with AChE via the same critical residues—Tyr72, Tyr124, Asp74, and Trp286—forming stable binding conformations that support effective enzyme inhibition [16]. This interaction likely contributes to cholinergic anti-inflammatory reflex activation, enhancing anti-inflammatory responses independently of sPLA$_2$ modulation. For COX-2, CP2 occupied the catalytic cavity with robust interactions involving Ser353 and Tyr355, maintaining proximity to the heme group

in a manner similar to CP1 [12]. This binding pattern suggests effective prostaglandin synthesis inhibition, contributing significantly to the observed anti-inflammatory efficacy (Figure 5).

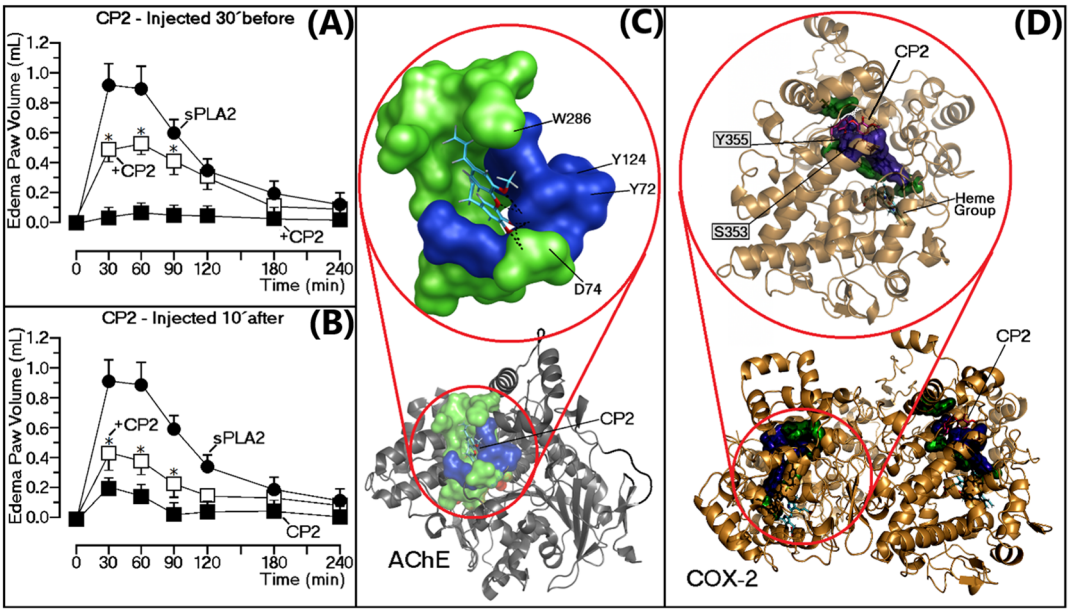



**Figure 5.** Comparative analysis of CP2 multitarget activity. (**A**,**B**) Anti-inflammatory efficacy comparable to CP1 despite modest sPLA2 inhibition. (**C**) AChE binding showing similar interaction pattern to CP1. (**D**) COX-2 binding demonstrating effective active site occupation and heme group proximity. * $p$-values < 0.05.

The combined enzymatic, in vivo, and computational results demonstrate that CP1 and CP2 exert their anti-inflammatory effects through an integrated multitarget mechanism involving three complementary pathways [1]:

1. Partial $sPLA_2$ modulation through active site and calcium binding loop interactions, reducing catalytic efficiency and arachidonic acid release [11].
2. Neuroimmune regulation via AChE inhibition, leading to acetylcholine accumulation and activation of the cholinergic anti-inflammatory reflex, which suppresses pro-inflammatory cytokine release [16].
3. Prostaglandin synthesis blockade through COX-2 inhibition, effectively preventing the formation of key inflammatory mediators responsible for edema, pain, and fever [12].

This multitarget strategy provides significant pharmacological advantages over traditional single-target approaches, offering broader efficacy by intervening at multiple critical points in the inflammatory cascade [2]. The ability of these compounds to potentially disrupt lipid membrane organization introduces a novel interfacial inhibition paradigm that may enhance selectivity and reduce resistance development [7]. The exceptional experimental–computational correlation ($R^2$ = 0.89) validates the quantitative docking approach as a reliable tool for predicting multitarget activity and provides a robust framework for future compound optimization [8]. The clear structure–activity relationships identified through this analysis offer valuable insights for designing next-generation anti-inflammatory agents with enhanced potency and selectivity. These findings position CP1 and CP2 as promising lead compounds for developing multitarget anti-inflammatory therapies, particularly for complex inflammatory conditions where single-target interventions might be insufficient [15]. In studies conducted in rats, the pharmacokinetic profile after a single dose showed adequate parameters to support further in vivo studies aimed at validating its efficacy [13]. Their natural origin, combined with validated multitarget

profiles and excellent safety margins, enhances their potential as nutraceuticals, botanical drugs, or pharmaceutical agents for treating inflammatory diseases.

## 3. Materials and Methods

### *3.1. Compounds and Reagents*

Dehydrodieugenol (CP1) and dehydrodieugenol B (CP2) were isolated from leaves of *Nectandra leucanta* and characterized by NMR and mass spectrometry (Supplementary Material), as previously described [10]. Additional derivatives CP3, CP4, and CP5 were synthesized following established protocols [14]. sPLA2 was purified from *Crotalus durissus terrificus* venom using established chromatographic protocols. The chromogenic substrate 4-nitro-3-octanoyloxy-benzoic acid (NOBA) was obtained from Sigma-Aldrich (St. Louis, MO, USA).

### *3.2. Enzymatic Assays*

sPLA2 activity was measured using the chromogenic substrate NOBA, which was dissolved in acetonitrile (100%). The purified sPLA2 had its concentration adjusted to 1 mg/mL and was added to 175 µL of buffer. The samples were incubated in 96-well plates at room temperature at 405 nm on a microplate reader, following established protocols. Reactions vessels contained 10 mM Tris-HCl buffer (pH 8.0), 10 mM $CaCl_2$, 100 mM NaCl, 0.32 mM NOBA, and varying concentrations of test compounds (1–100 µM). Initial velocity measurements (V0) were recorded, and the reaction was monitored for over 60 min at 37 °C. Inhibition patterns were analyzed using Lineweaver–Burk plots to determine inhibition type and kinetic parameters.

### *3.3. In Vivo Anti-Inflammatory Studies*

Male Swiss mice (25–30 g) were obtained from the Central Animal Facility and maintained under standardized laboratory conditions, food available always, light control, and a stable temperature of 28 °C. All experimental procedures were approved by the institutional ethics committee (ANIMAL USE ETHICS COMMITTEE—CEUA, of the institute of biosciences, coast of São Paulo campus, at a meeting on 7 May 2025 Protocol n° 02/2025). sPLA2-induced paw edema was performed, following previous protocols [19]. Treated mice received intraplantar injection of sPLA2 (10 µg/50 µL saline) in the right hind paw. Test compounds (50 mg/kg) were administered intraperitoneally either 30 min before (prophylactic protocol) or 10 min after (therapeutic protocol) sPLA2 injection. Paw volume was measured using a digital hydropletismometer at 15, 30, 60, 90 and 120 min post-injection.

### *3.4. Quantitative Molecular Docking Analysis*

Comprehensive computational analysis was performed using four independent docking algorithms, Piecewise Linear Potential (PLP), Astex Statistical Potential (ASP), ChemScore, and GoldScore, implemented in GOLD Suite v2022.1. Crystal structures were obtained from the Protein Data Bank: acetylcholinesterase (AChE, PDB: 1EVE), cyclooxygenase-2 (COX-2, PDB: 5KIR), and sPLA2 from *Crotalus durissus terrificus* in monomeric form (Mcdt, PDB: 1PA0) and quaternary form (Tcdt, homology model based on 1PA0). Ligand structures were optimized using Density Functional Theory (DFT) calculations at the B3LYP/6-31G(d,p) level using Gaussian16. Binding site definition included all residues within 10 Å of the active site. For each target, 100 independent genetic algorithm docking runs were performed for exhaustive sampling. Consensus scoring was applied to eliminate function-specific bias, and results were validated against known inhibitors: 1YL for AChE, meclofenamic acid for COX-2, and AYZ for sPLA2.

### *3.5. Statistical Analysis*

Data is presented as median (interquartile range) from at least three technical replicates. Statistical significance between control and treatment groups was determined using the Mann–Whitney U test. Time-dependent enzymatic activity was analyzed using the Friedman test. Correlation analysis between percentage of paw edema reduction and docking score was performed using the Pearson correlation coefficient. $p$-values < 0.05 were considered statistically significant.

## 4. Conclusions

This study establishes dehydrodieugenol neolignans as exceptional multitarget anti-inflammatory agents with significant therapeutic potential for complex inflammatory diseases. The comprehensive quantitative computational analysis using four independent docking algorithms provides unprecedented validation of the multitarget mechanism, with an exceptional correlation between paw edema reduction and docking scores ($R^2$ = 0.89, $p$ < 0.01), representing high consistency within the data. CP1 emerged as the lead compound, demonstrating optimal binding scores across all molecular targets (AChE: 78.5, COX-2: 83.8, sPLA2: 82.7–83.4) and achieving remarkable in vivo anti-inflammatory efficacy (68.3% edema reduction). The mechanistic integration reveals three convergent pathways: (1) partial sPLA2 modulation through active site interactions, (2) neuroimmune regulation via AChE inhibition activating the cholinergic anti-inflammatory reflex, and (3) prostaglandin synthesis blockade through COX-2 inhibition. The quantitative structure–activity relationships identified critical molecular features for multitarget activity, including methoxy groups, phenolic OH groups, and allyl side chains, providing valuable insights for future compound optimization. The clear separation between active (CP1, CP2) and inactive (CP3-CP5) compounds validates the computational approach and establishes robust design principles for next-generation anti-inflammatory agents. This multitarget approach offers significant advantages over traditional single-target strategies, providing broader therapeutic efficacy while potentially reducing side effects and resistance development. The natural origin of these compounds, combined with their validated multitarget profiles and excellent experimental–computational correlation, positions them as promising candidates for developing innovative therapies against complex inflammatory diseases. Future studies should focus on pharmacological optimization, detailed safety evaluation, and clinical translation to fully realize the therapeutic potential of these remarkable natural products in treating inflammatory conditions that remain challenging for current therapeutic approaches.

**Supplementary Materials:** The following supporting information can be downloaded at: https://www.mdpi.com/article/10.3390/ddc5010020/s1, Dehydrodieugenol; Dehydrodieugenol B; Dehydrodieugenol B methyl ether; 7-Hydroxy-dehydrodieugenol B; 7-Hydroxy-dehydrodieugenol B methyl ether [10,20]; Figure S1: $^{1}$H NMR spectrum of dehydrodieugenol (δ, $CDCl_3$, 300 MHz); Figure S2: $^{13}$C NMR spectrum of dehydrodieugenol (δ, $CDCl_3$, 75 MHz); Figure S3: ESI-HRMS spectrum of dehydrodieugenol; Figure S4: $^{1}$H NMR spectrum of dehydrodieugenol B (δ, $CDCl_3$, 300 MHz); Figure S5: $^{13}$C NMR spectrum of dehydrodieugenol B (δ, $CDCl_3$, 75 MHz); Figure S6: ESI-HRMS spectrum of dehydrodieugenol B. Figure S7: $^{1}$H NMR spectrum of dehydrodieugenol B methyl ether (δ, $CDCl_3$, 300 MHz); Figure S8: $^{13}$C NMR spectrum of dehydrodieugenol B methyl ether (δ, $CDCl_3$, 75 MHz); Figure S9: ESI-HRMS spectrum of dehydrodieugenol B methyl ether; Figure S10: $^{1}$H NMR spectrum of 7-hydroxy-dehydrodieugenol B (δ, $CDCl_3$, 300 MHz); Figure S11: $^{13}$C NMR spectrum of 7-hydroxy-dehydrodieugenol B (δ, $CDCl_3$, 75 MHz); Figure S12: ESI-HRMS spectrum of 7-hydroxy-dehydrodieugenol B; Figure S13: $^{1}$H NMR spectrum of 7-hydroxy-dehydrodieugenol B methyl ether (δ, $CDCl_3$, 300 MHz); Figure S14: $^{13}$C NMR spectrum of 7-hydroxy-dehydrodieugenol B methyl ether (δ, $CDCl_3$, 75 MHz); Figure S15: ESI-HRMS spectrum of 7-hydroxy-dehydrodieugenol

B methyl ether; Figure S16: Representative HPLC chromatogram of the dehydrodieugenol (CP1) obtained using a C5 column with detection at 280 nm; Figure S17: Representative HPLC chromatogram of the dehydrodieugenol B (CP2) obtained using a C5 column with detection at 280 nm; Figure S18: Representative HPLC chromatogram of the dehydro-dieugenol B methyl ether (CP3) obtained using a C5 column with detection at 280 nm; Figure S19: Representative HPLC chromatogram of the 7-hydroxy-dehydrodieugenol B (CP4) obtained using a C5 column with detection at 280 nm; Figure S20: Representative HPLC chromatogram of the 7-hydroxy-dehydrodieugenol B methyl ether (CP5) obtained using a C5 column with detection at 280 nm; Table S1: Comprehensive Quantitative Docking Scores for All Compounds and Targets; Table S2: Multi-Algorithm Consensus Analysis; Table S3: Structure–Activity Relationship Analysis; Table S4: Experimental vs. Computational Correlation Analysis.

**Author Contributions:** Conceptualization, methodology and writing—original draft preparation, M.H.T., C.R.C.C. and A.B.S.J.; Validation and Conceptualization, M.H.T. and C.R.C.C.; Data curation, M.A.O., J.H.G.L. and S.F.S.; Editing and software, A.R. and I.N.O.; Assistance in Biological Assays, D.R.S.L., P.P.B. and W.H.B.C.S.; Visualization, supervision, project administration, M.H.T. All authors have read and agreed to the published version of the manuscript.

**Funding:** This research was funded by CNPq (Process 442831/2023-4/Projetos Int 2023) and FAPESP (Process 17/20291-0 and 25/04557-7).

**Institutional Review Board Statement:** The animal study protocol was approved by the ANIMAL USE ETHICS COMMITTEE (CEUA) OF THE INSTITUTE OF BIO SCIENCES, COAST OF SÃO PAULO CAMPUS, UNESP, at a meeting on 7 May 2025 (n° 02/2025).

**Data Availability Statement:** All contributions to this study are original and are available in the article and Supplementary Material. For more information, please contact the corresponding author.

**Acknowledgments:** The authors thank the São Paulo Research Foundation (FAPESP) and the National Council for Scientific and Technological Development (CNPq) for financial support. We acknowledge the computational resources provided by the National Laboratory for Scientific Computing (LNCC) for molecular modeling studies and the Central Animal Facility for providing experimental animals. This work received financial support from the PT national funds (FCT/MECI, Fundação para a Ciência e Tecnologia and Ministério da Educação, Ciência e Inovação) through the project UID/50006-Laboratório Associado para a Química Verde-Tecnologias e Processos Limpos. The authors are also thankful to the EuroHPC Joint Undertaking for awarding this project access to the EuroHPC supercomputer LUMI, hosted by CSC (Finland) and the LUMI consortium through a EuroHPC Regular Access call.

**Conflicts of Interest:** The authors declare no conflicts of interest.

## References

1. Anighoro, A.; Bajorath, J.; Rastelli, G. Polypharmacology: Challenges and opportunities in drug discovery. *Clin. Transl. Med.* **2014**, *3*, 6. [CrossRef] [PubMed]
2. Newman, D.J.; Cragg, G.M. Natural products as sources of new drugs over the nearly four decades from 01/1981 to 09/2019. *J. Nat. Prod.* **2020**, *83*, 770–803. [CrossRef] [PubMed]
3. Dennis, E.A.; Cao, J.; Hsu, Y.H.; Magrioti, V.; Kokotos, G. Phospholipase A2 enzymes: Physical structure, biological function, disease implication, chemical inhibition, and therapeutic intervention. *Chem. Rev.* **2011**, *111*, 6130–6185. [CrossRef] [PubMed]
4. Murakami, M.; Taketomi, Y.; Miki, Y.; Sato, H.; Hirabayashi, T.; Yamamoto, K. Recent progress in phospholipase A2 research: From cells to animals to humans. *Adv. Immunol.* **2011**, *132*, 87–162. [CrossRef] [PubMed]
5. Burke, J.E.; Dennis, E.A. Phospholipase A2 structure/function, mechanism, and signaling. *J. Biol. Chem.* **2009**, *297*, 101875. [CrossRef] [PubMed]
6. Lambeau, G.; Gelb, M.H. Biochemistry and physiology of mammalian secreted phospholipases A2. *Methods Enzymol.* **2008**, *583*, 159–186. [CrossRef] [PubMed]
7. Gelb, M.H.; Jain, M.K.; Hanel, A.M.; Berg, O.G. Interfacial enzymology of glycerolipid hydrolases: Lessons from secreted phospholipases A2. *Annu. Rev. Biochem.* **1995**, *64*, 653–688. [CrossRef] [PubMed]

8. Teponno, R.B.; Kusari, S.; Spiteller, M. Recent advances in research on lignans and neolignans. *Nat. Prod. Rep.* **2016**, *33*, 1044–1092. [CrossRef] [PubMed]
9. Galhardo, T.S.; Ueno, A.K.; Costa-Silva, T.A.; Tempone, A.G.; Carvalho, W.A.; Fischmeister, C.; Bruneau, C.; Mandelli, D.; Lago, J.H.G. New derivatives from dehydrodieugenol B and its methyl ether displayed high anti-Trypanosoma cruzi activity and cause depolarization of the plasma membrane and collapse the mitochondrial membrane potential. *Chem.-Biol. Interact.* **2022**, *366*, 110129. [CrossRef] [PubMed]
10. Grecco, S.S.; Costa-silva, T.A.; Jerz, G.; Sousa, F.S.; Londero, V.S.; Gallupo, M.C.; Lima, M.L.; Neves, B.J.; Andrade, C.H.; Tempone, A.G.; et al. Neolignans from leaves of *Nectandra leucantha* (*Lauraceae*) display in vitro antitrypanosomal activity via plasma membrane and mitochondrial damages. *Chem.-Biol. Interact.* **2017**, *277*, 55–61. [CrossRef] [PubMed]
11. Balsinde, J.; Winstead, M.V.; Dennis, E.A. Phospholipase A2 regulation of arachidonic acid mobilization. *FEBS Lett.* **2002**, *1761*, 1373–1382. [CrossRef] [PubMed]
12. Bittencourt-Mernak, M.I.; Pinheiro, N.M.; Silva, R.C.; Ponci, V.; Banzato, R.; Pinheiro, A.J.M.C.R.; Olivo, C.R.; Tibério, I.F.L.C.; Neto, L.G.L.; Santana, F.P.R.; et al. Effects of Eugenol and Dehydrodieugenol B from *Nectandra leucantha* against Lipopolysaccharide (LPS)-Induced Experimental Acute Lung Inflammation. *J. Nat. Prod.* **2021**, *84*, 2282–2294. [CrossRef] [PubMed]
13. Amaral, M.; Romanelli, M.M.; Asiki, H.; Bicker, J.; Lage, D.P.; Freitas, C.S.; Taniwaki, N.N.; Lago, J.H.G.; Coelho, E.A.F.; Falcão, A.; et al. Synthesis of a dehydrodieugenol B derivative as a lead compound for visceral leishmaniasis-mechanism of action and in vivo pharmacokinetic studies. *Antimicrob. Agents Chemother.* **2024**, *68*, 18. [CrossRef] [PubMed]
14. Sear, C.E.; Pieper, P.; Amaral, M.; Romanelli, M.; Costa-Silva, T.A.; Haugland, M.M.; Tate, J.A.; Lago, J.H.G.; Tempone, A.G.; Anderson, E.A. Structure-activity relationships of dehydrodieugenol derivatives against Trypanosoma cruzi. *ACS Infect. Dis.* **2020**, *6*, 2872–2878. [CrossRef] [PubMed]
15. Murakami, M.; Lambeau, G. Emerging roles of secreted phospholipase A2 enzymes: An update. *Biochimie* **2013**, *95*, 43–50. [CrossRef] [PubMed]
16. Tracey, K.J. The inflammatory reflex. *Nature* **2002**, *420*, 853–859. [CrossRef] [PubMed]
17. Salvador, G.H.M.; Gomes, A.A.S.; Bryan-Quirós, W.; Fernández, J.; Lewin, M.R.; Gutiérrez, J.M.; Lomonte, B.; Fontes, M.R.M. Structural basis for phospholipase A2-like toxin inhibition by the synthetic compound Varespladib (LY315920). *Sci. Rep.* **2019**, *9*, 17203. [CrossRef] [PubMed]
18. Roggero, A.; Loyola, P.M.; Cruz, C.R.; Santos, W.H.B.C.; Borges, P.P.; Santos Junior, A.B.; Martins, F.; Oliveira, M.A.; Sousa, S.F.; Toyama, M.H. NSAIDs beyond COX: In Silico and In Vitro Insights into Acetylcholinesterase Modulation. *ACS Omega* **2025**, *10*, 56617–56629. [CrossRef] [PubMed]
19. dos Santos Junior, A.B.; Tamayose, C.I.; Ferreira, M.J.P.; Belchor, M.N.; Costa, C.R.C.; de Oliveira, M.A.; Toyama, M.H. Bioaffinity Fishing Procedure Using Secretory Phospholipase A2 for Screening for Bioactive Components: Modulation of Pharmacological Effect Induced by sPLA2 from *Crotalus durissus terrificus* by Hispidulin from *Moquiniastrum floribundum*. *Molecules* **2020**, *25*, 282. [CrossRef] [PubMed]
20. Grecco, S.S.; Costa-Silva, T.A.; Sousa, F.S.; Conserva, G.A.A.; Jerz, G.; Mesquista, J.T.; Gallupo, M.C.; Tempone, A.G.; Neves, B.J.; Andrade, C.H.; et al. Antitrypanosomal activity and evaluation of the mechanism of action of dehydrodieugenol isolated from *Nectandra leucantha* (Lauraceae) and its methylated derivative against Trypanosoma cruzi. *Phytomedicine* **2017**, *24*, 62–67. [CrossRef] [PubMed]


**Disclaimer/Publisher's Note:** The statements, opinions and data contained in all publications are solely those of the individual author(s) and contributor(s) and not of MDPI and/or the editor(s). MDPI and/or the editor(s) disclaim responsibility for any injury to people or property resulting from any ideas, methods, instructions or products referred to in the content.